Seasonality of fluorescent particles in the Arctic

Margarida Teles Nogueira Rolo
margaridarolo@tecnico.ulisboa.pt

Instituto Superior Técnico, Lisboa, Portugal
November 2021

Abstract

One of the most sensitive regions to climate change is the Arctic and these alterations are coming faster than ever and with a great intensity (Serreze & Barry, 2011). The surface air temperature, which is one of the most important variables to indicate these changes, increased two times faster in the Arctic comparing to the rest of the globe, since the mid of the 20th century. This phenomenon is called Arctic Amplification. Bioaerosols have importance in environmental systems. For instance, they play a role on the cloud formation. Recently, there has been an increase in the frequency of scientific publications using instruments based on ultraviolet laser/light-induced fluorescence (UV-LIF) like the WIBS (wideband integrated bioaerosol sensor) for bioaerosol detection. The WIBS was used in the Multidisciplinary drifting Observatory for the Study of Arctic Climate (MOSAiC) to measure fluorescent and total particle concentrations and particle size and shape. This data was analyzed and some of the final conclusions were that total particle concentrations are usually two orders of magnitude higher than the fluorescent particle concentrations. Moreover, both total and fluorescent particles have their highest median values of concentration in the December-January-February (DJF) and March-April-May (MAM) seasons, and the concentration peaks are reached in January and February. August and October are months with low values of concentrations. Regarding particle sizes, the conclusion to be taken is that fluorescent particles are generally the same size as non-fluorescent particles. Particle fractions were calculated, reaching the conclusion that AB type particles are clearly dominant in polluted periods. Finally, wind was seen as a possible mechanism to lift snow and sea particles, making them possible local sources of fluorescent bioaerosols.

Keywords: Arctic Amplification, Bioaerosols, Fluorescent Particles, MOSAiC, WIBS

Introduction

Aerosols and their importance. Why in the Arctic?

Several decades ago, the importance of aerosols started to be recognized as scientist came to realize they have a role in the oxidative capacity of the atmosphere, as well as cloud condensation (CCN) and ice-forming nuclei (IN). They can have some global and local impacts like climate change, toxicity and health hazards. Investigating the sources of this aerosols and how they can vary with time and space, has been an increasing need in these last few decades even though, particularly bioaerosols and their physical and chemical atmospheric processes, are still poorly understood.

Airborne particles or aerosols are important because they can directly (by absorbing or scattering radiation) or indirectly (related with their ability to form or act as CCN and IN, and hence lead to the formation of clouds, thus indirectly influencing the Earth's radiation budget) impact the Earth's climate (Ariya et al., 2009).

One of the most sensitive regions to climate change is the Arctic and these alterations are coming faster than ever and with a great intensity (Serreze & Barry, 2011). The surface air temperature, which is one of the most important variables to indicate these changes, increased two times faster in the Arctic comparing to the rest of the globe, since the mid of the 20th century (Overland et al., 2011; Serreze & Barry, 2011). This phenomenon is called Arctic Amplification,(Pithan & Mauritsen, 2014; Serreze & Barry, 2011).

Clouds are one of the key factors of Arctic Amplification since they affect the energy budget of the Arctic boundary layer. By reflecting long-wave radiation, they tend to warm the surface and therefore lead to sea ice melting (Vavrus et al., 2011), which will enhance the evaporation and cloud formation. This feedback will probably accelerate in the future**.** As the ice cover reduces, biological activity increases in the marine and terrestrial environment. This is related with the alteration of aerosol particle sources, that may affect clouds and their properties (Hartmann et al., 2019).

While in the past most of the attention on aerosol climatic effects went to long-range transported anthropogenic pollution (Arctic Haze) (Quinn et al., 2007; Schmale et al., 2021), nowadays, an emphasis on the inner-Arctic is starting to appear, especially when it comes to natural aerosol sources.

Fluorescent aerosols and their importance

Recently, there has been an increase in the frequency of scientific publications using instruments based on ultraviolet laser/light-induced fluorescence (UV-LIF), such as the WIBS (wideband integrated bioaerosol sensor) or UV-APS (ultraviolet aerodynamic particle sizer), for bioaerosol detection both outdoors and in the built environment. Some problems, despite all the efforts, have occurred when it comes to characterize the particles and understand which are from biological origin and which are not. These gaps in the current knowledge are caused by the detection ability of LIF instrumentation (Moallemi et al., 2021; Savage et al., 2017). The wavelength detection ranges are chosen to match regions of fluorescence for biological compounds that are found ubiquitously in bioaerosols, such as tryptophan and Nicotinamide Adenine Dinucleotide (NADH) (Savage et al., 2017).

Changing the particle fluorescence threshold was shown to have a significant impact on fluorescence fraction and particle type classification. However, raising the fluorescence threshold has no impact in reducing the relative fraction of biological material considered fluorescent but can significantly decrease the interference from mineral dust and other non-biological aerosols. Some examples of highly fluorescent interfering particles are brown carbon, soot and cotton fibers (Savage et al., 2017).

Contributors to fluorescent signals: biological particles and interference from dust and Black Carbon

Bioaerosols are airborne particles or large molecules that range between 1 - 10 nm and 100 um diameter and originate from multiple sources in nature. They are considered a subgroup of biogenic organic aerosols. They can be found alive, dead, dormant or like products released from living organism. Some examples of these particles are bacteria, viruses, fungi, metabolites, pollen, cell debris and biofilms, and these might be emitted by biogenic sources such as oceans, vegetation, soils, lakes, and living organisms (Ariya et al., 2009). It is yet to be known if they have a major contribution in the overall organic aerosol budget. In the likes of other aerosol particles, the ice nucleation ability varies depending on the type of particle and the importance they have changes with the tropospheric concentrations (Ariya et al., 2009).

The concentration of these particles varies with the temperature, radiation, relative humidity, rainfall, and wind speed and direction, as well as other seasonal

factors such as fungal spores or airborne bacteria concentration (gram-positive and gram-negative), in the form of single spores or clusters.

Biological particle signatures have already been detected in some ice residues sampled from clouds, but it is still uncertain what is their impact concerning regional and global scale cloud formation.

Mineral dust has been recognized as a major contributor to atmospheric ice nucleation at temperatures relevant for mixed phase and cirrus clouds (Heintzenberg et al., 1996) and it has the capacity of interfering with the detection of fluorescent particles.

Conventionally, black carbon (BC) or soot is considered as the main light absorber in atmospheric aerosols over the spectrum ranging from ultraviolet to infrared (Wu et al., 2020) and it has the same ability of interfering with fluorescent aerosols measurements as dust does. Soot is a black material found in smoke from wood and coal fires and it has been seen as the main representative air pollutant throughout history (Andreae & Gelencsér, 2006).

Methods

Campaign Description

The Multidisciplinary drifting Observatory for the Study of Arctic Climate (MOSAiC) is the most extensive expedition in the central Arctic Ocean. Embarked on the German research vessel RV Polarstern, the largest polar expedition in history took place from September 2019 to October 2020. The icebreaker set sail from Tromsø, Norway, to spend a year drifting through the Arctic Ocean - trapped in ice (MOSAiC Consortium, 2016) ending the expedition in October 2020 in Bremerhaven, Germany.

The scientific work in MOSAiC was executed on the ship itself and on the ice around the ship. A full annual cycle of observations was accomplished.

During the expedition a laboratory container was running on the ship, equipped with several instruments, to measure aerosol concentration, size distribution and their chemical composition. A research camp was set up on the ice around the ship.

Fluorescent Aerosol Measurements

The Wideband Integrated Bioaerosol Sensor-New Electronics Option (WIBS-NEO - originally developed by the University of Hertfordshire and is licensed to and manufactured by Droplet Measurement Technologies) was used to measure fluorescent aerosol particles on a single-particle basis. Furthermore, the WIBS measures aerosol optical diameter in a range of sizes between 0.5 and 50 μm, and asymmetry factor (AF) which is a measure of aerosol morphology. In order to excite fluorescence in individual particles, the instrument uses UV xenon flashlamp sources. Contrasting with UV lasers, the UV xenon flashlamp sources allow for the precise selection of particular UV wavebands. These wavebands were selected to optimize the detection of the common bioaerosol components (Tryptophan and nicotinamide adenine dinucleotide - NADH) on the WIBS-NEO.

Fluorescent Particle Detection

The aerosol fluorescent measurements are conducted by exciting particles with two Xenon flash lamps at wavelengths of 280 and 370 nm and then detecting the fluorescent light intensity in the wavebands from 310-400 nm and 420–650 nm. This results in three different excitation wavelength (ExWL) and emission waveband (EmWB) configurations: channel A (ExWL 280 nm and EmWB 310–400 nm), channel B (ExWL 280 nm and EmWB 420–650 nm) and channel C (ExWL 370 nm and EmWB 420–650 nm). The fluorescent detection threshold in each channel is determined based on the background signal measured during a “forced triggering” (FT) procedure. Moreover, we use the classification scheme introduced by Perring et al. (2015). In this method, the fluorescent particles are divided into 7 different classes (A, B, C, AB, AC, BC, and ABC) based on the logical combination of emitted signals in the three fluorescent channels (Moallemi et al., 2021).

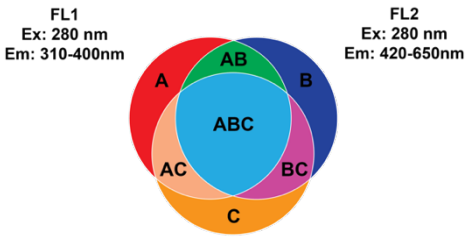

Figure 1. Fluorescent particles classes (Adapted from *Droplet Measurement Technologies, n.d.)*.

WIBS-NEO Toolkit

The WIBS-NEO Toolkit is data analysis software for the WIBS-NEO Instrument, developed using IGOR. This tool is used to load, process, visualize, and inspect data generated by the WIBS-NEO.

Functionality includes loading single and multiple raw data files containing particle-by-particle fluorescence, size, asymmetry factor and other particle-relevant data. The software then converts particle-by-particle data into time-resolved particle concentrations, and size distributions (Droplet Measurement Technologies, n.d.).

In this study, the toolkit was used to load raw data files that were organized in monthly periods and extract .csv monthly files with different particle data.

Data Analysis

Concerning the data analyzis, it was first used IGOR PRO 8, version 8.0.4.2, 64 bit, by WaveMetrics, along with the WIBS-NEO toolkit, to process the WIBS data.

Firstly, all the raw data files and forced trigger files were joined in different folders, separated by month. The toolkit provides options for loading all files in a single directory or for loading a single file within a directory. These folders were loaded in IGOR on the *Load data and Background* window, using the option *Load all files in folder* for both the raw data and the forced trigger background. Subsequently, the data was saved as a text file by selecting the button on the main Toolkit screen. The monthly text files (.csv) provided data for average asphericity, average size (μm) and average concentration (cm^3), for all types of particles, in one second resolution. These text files were then concatenated into a single dataset using Python.

Afterward, a pollution mask developed by Beck et al. (in preparation) was applied to the dataset. This pollution mask uses Condensation Particle Counter (CPC) data. The periods that have really high concentrations or concentration above the median or the gradient, are deleted. When applied to the WIBS dataset, 0 corresponds to polluted periods and 1 to clean periods. The dataset was then separated into polluted data and clean data.

The weather is also an important factor which influences aerosol concentrations. Wind data was collected during the entire expedition on Polarstern. Wind speed and direction were measured with a 2D sonic anemometer on the main mast of the vessel. The wind dataset was used in a time resolution of 1 minute in this study.

Results and Discussion

Fluorescent particle concentrations throughout the year

In this first chapter, seasonal particle concentrations will be approached.

Figure 2 shows the seasonal variation of both total and fluorescent particle concentration in a linear axis. The difference between total concentration and fluorescent concentration is demonstrated in figure 2 and it can be observed that the first can reach sometimes two orders of magnitude higher than the second.

For total particle concentration, highest medians (medians give us information about the mid-point of the data, meaning that 50% of the data will be below that point and the other 50% will be above) occur from November to May and the greatest concentrations happen in January and February. In summer months and October, there are lower medians and concentrations, reaching its lowest values in August and October. As for the fluorescent particle concentrations, they follow the same pattern as the total particle concentrations, the peaking in January and February and having their lowest medians and concentrations in August and October.

The highest concentration of total particles is about 15 particles per cm^3 in February, reaching in the same month the highest median as well, with a value of 4 particles per cm^3. Contemplating the fluorescent particle concentrations, the maximum concentration is around 0.40 particles per cm^3 in January and the median is 0.15 particles per cm^3.

On the other hand, summer and autumn seasons have low concentrations, both in total and fluorescent particles. October and August reach concentrations of almost 0 particles per cm^3.

When considering the Arctic Haze phenomenon, these results make sense since this phenomenon is amplified in winter and spring seasons, when the long-range transport of pollutant aerosols is higher. Even though in summer months there are more forest fires, this is not enough to surpass what happens in winter or spring seasons (Quinn et al., 2007).

When contemplating fluorescent concentrations, one would expect to have higher concentrations in summer, since, in principle, these should be the months when biological activity is more intense and therefore, bioaerosols would be in greater representation. One hypothesis is that, during winter/springtime, particles that can interfere with the fluorescence detection like

dust or black carbon, are more dominant. To confirm this, one could look into pollution data (black carbon data, for example) and try to relate this concentrations with the previous data, in each month.

To complement the previous hypotheses, studies on back trajectory data could be made, in order to understand where the particles could be coming from and also, looking into some specific case studies (like storms, for example) in deeper detail to have an idea of how they can influence the concentrations of fluorescent and non-fluorescent particles.

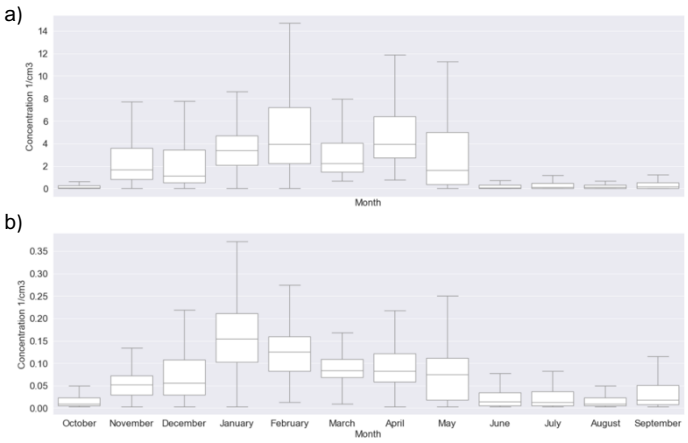

Figure 2. Seasonal variation in linear axis. a) Total particle concentration. b) Fluorescent particles concentration as measured by the WIBS.

Seasonality of particles size

These second chapter has the purpose of discussing the difference in sizes over the year. For that, the boxplots in figure 3 were plotted.

In the boxplots below, it is possible to see that the median sizes are similar throughout the year, even though, in winter and spring, the maximum sizes are smaller than in summer and autumn. The variation of sizes is minor in winter and in spring and in summer and autumn, it is bigger. The largest particles in figure 3 a) measure around 1.27 μm in June and the smallest around 0.5 μm (this is the lower limit of the instrument). As for the sizes of the fluorescent particles, they are generally the same size as the rest of the particles. The biggest particles measure about 1.9 μm in October and the smaller ones are again 0.5 μm. These results suggest that non-fluorescent particles have a smaller size distribution than the fluorescent ones.

Dust and combustion particles have a greater range of sizes than biogenic particles. However, since the variation of sizes in the absence of biological activity (winter months) and keeping in mind that the maximum sizes are smaller in the winter and spring, one of the possible hypotheses is that bioaerosols are generally bigger than other types of particles in the Arctic.

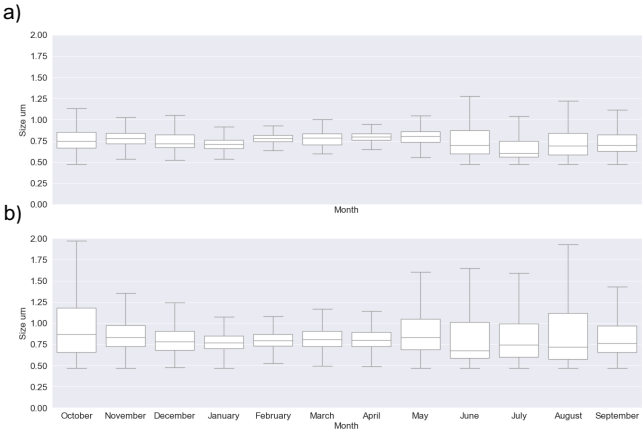

Figure 3. Seasonal variation in linear axis. a) Total particle size. b) Fluorescent particles size as measured by the WIBS.

Figure 4 aims the deep clarification of the boxplots above with the binning of the different sizes.

In figure 4 it can be seen that sizes between 0.7 and 0.9 μm are dominant, meaning they have higher concentrations, with medians of approximately 0.09 particles per cm^3 and maximums ranging between 0.27 and 0.29 particles per cm^3. These two size ranges are the sizes with more datapoints (table 1), meaning they are more representative.

The typical size range of bacteria is between 0.5-6 μm. In figure 4, the size range of the particles is exactly this size range, leading to the conclusion that these results reflect a majority of biogenic particles.

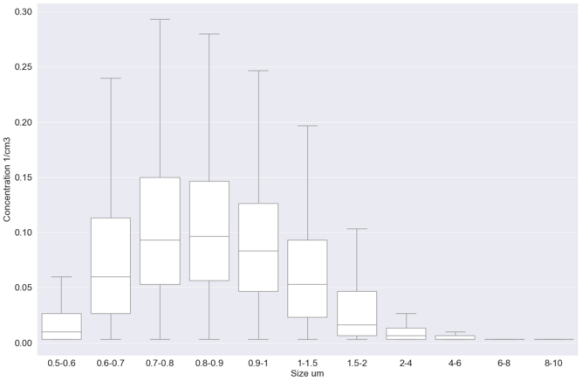

Figure 4. Variation of sizes of fluorescent particles.

Table 1. Number of datapoints on each size bin of fluorescent particles.

Size Range	Number of datapoints
0.5 – 0.6	13343
0.6 – 0.7	28885
0.7 – 0.8	41285
0.8 – 0.9	32164
0.9 – 1.0	17685
1.0 – 1.5	20585
1.5 – 2.0	3360
2.0 – 4.0	2210
4.0 – 6.0	234
6.0 – 8.0	66
8.0 – 10.0	26

In figure 5 it can be seen that sizes between 0.8 and 1 μm are dominant, meaning they have higher concentrations, with medians of approximately 4.5 and 2.5 particles per cm^3 and maximums ranging between 15 and 16.1 particles per cm^3. The three size ranges with more datapoints (table 2) and therefore, more representative are the sizes between 0.6 – 0.9 μm.

In this case, the results in question are for all particles data, suggesting this way that when mixing non-fluorescent particles with fluorescent particles, the concentrations are higher in each size range but there are fewer size ranges.

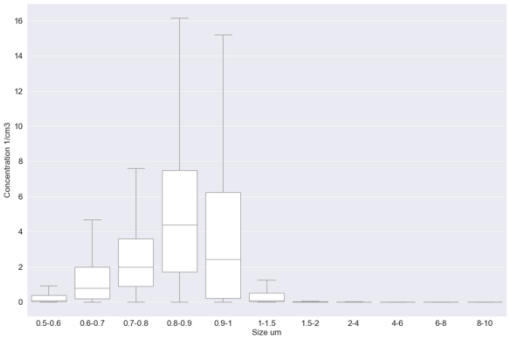

Figure 5. Variation of sizes of total particles.

Table 2. Number of datapoints on each size bin of total particles.

Size Range	Number of datapoints
0.5 – 0.6	15569
0.6 – 0.7	41577
0.7 – 0.8	62555
0.8 – 0.9	42983
0.9 – 1.0	9896
1.0 – 1.5	4961
1.5 – 2.0	539
2.0 – 4.0	426
4.0 – 6.0	65
6.0 – 8.0	23
8.0 – 10.0	11

Particle fractions

In order to understand if the different particle types have different patterns over the year, two graphs were plotted: one for clean periods only (figure 6) and one for polluted periods only (figure 7). In these graphs, the colors correspond to fluorescent particles of different types.

The first thing that figure 6 shows is that the AB and B type particles seem to be overall the dominant types in clean periods. Both types are more preeminent during the summer months. The AC particles are the ones with the smallest fraction.

The biggest AB fraction and the smallest B fraction happen in June and the biggest B fraction and smallest AB fraction happen in January.

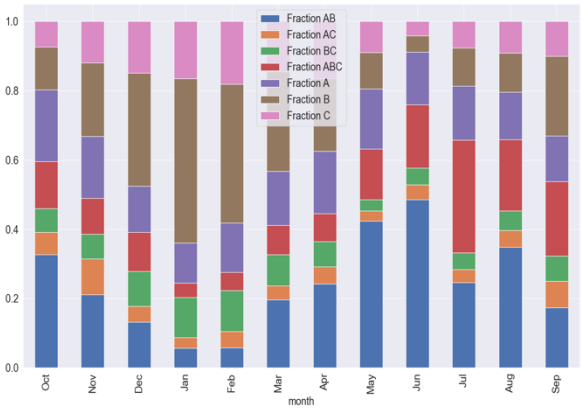

Figure 6. Seasonal variation of fractions of the different types of particles during clean periods.

When looking at figure 7, there is a clear conclusion: AB particles are the dominant particles in pollution periods and they are more present throughout the year. Then again, the AC particles are the ones with the negligible fraction. Figure 7 establishes that pollution is clearly a source of fluorescent particles. December, January, February and March are the months with less AB type particles. April is month with more AB type particles.

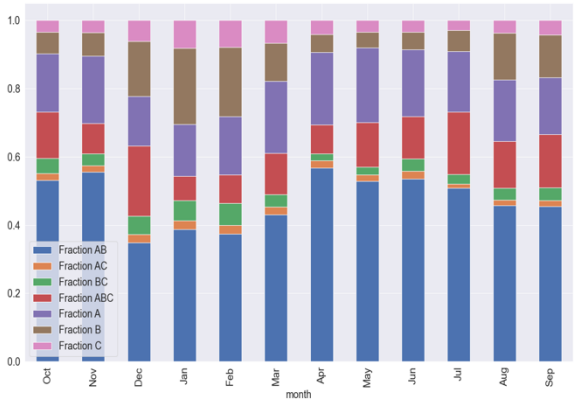

Figure 7. Seasonal variation of fractions of the different types of particles during polluted periods.

To support the hypothesis (Moallemi et al., 2021) that AB particles are dominant in pollution, the following equations were calculated:

$$\frac{Mean\ Concentration\ of\ AB\ particles\ despiked}{Mean\ Concentration\ of\ All\ particles\ despiked} = \frac{0.0193}{2.9772} = 0.0065$$

$$\frac{Mean\ Concentration\ of\ AB\ particles\ polluted}{Mean\ Concentration\ of\ All\ particles\ polluted} = \frac{0.1655}{2.6041} = 0.0636$$

As shown, the presence of AB particles in pollution in one order of magnitude higher then clean periods. This hypothesis would benefit from more studies in different regions of the planet, to confirm that in pollutes sites, there's always a dominance of AB type particles over the other types.

Potential Sources

It is proven now that pollution is one of the potential sources for fluorescent particles. But it is conceivable that other sources may exist. These sources can be snow (the wind as an uplifting mechanism of snow) or other local sources and possible regional sources.
The boxplot from figure 8 intends to show the influence of the wind in the concentration of fluorescent particles. Figure 8 represents the full year cycle. The medians increase with the wind speed until the 16 m/s and then they start to decrease, meaning that wind has in fact some effect in the increasing of concentrations.
Most of the datapoints (table 3) are from the lower concentrations, meaning that lower speeds are much more represented than higher speeds.
This result is related to a possible local source, using wind as a mechanism but, to really have the full extent of the possible sources, back trajectory data would have to be used to evaluate regional sources, instead of just local, since there's also a high probability of particles coming to the Arctic from the north of Europe.

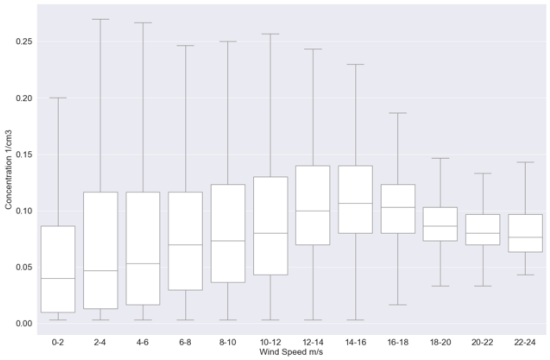

Figure 8. Concentration of fluorescent particles as a function of wind speed (full year cycle).

Table 3. Number of datapoints on each wind speed bin (full year).

Wind Speed Range	Number of datapoints
0 – 2	7921
2 – 4	29209
4 – 6	41008
6 – 8	46260
8 – 10	28839
10 – 12	18101
12 – 14	11048
14 – 16	5239
16 – 18	1507
18 – 20	417
20 – 22	279
22 – 24	85

Conclusions

Some conclusions on the seasonality of fluorescent particles were taken. Total and fluorescent particle concentrations were discussed and led to the inference that total particle concentrations are usually two orders

of magnitude higher than the fluorescent particle concentrations. Moreover, both total and fluorescent particles have their highest median values of concentration in the December-January-February (DJF) and March-April-May (MAM) seasons, and the concentration peaks are reached in January and February. August and October are months with low values of concentrations. This can be explained by the Arctic Haze phenomenon, although the expectation was that the summer would have higher concentrations of fluorescent particles due to the increased biological activity.

Regarding particle sizes, the median sizes are similar throughout the year, but June-July-August (JJA) and September-October-November (SON) seasons have the bigger maximum sizes. Considering the size measures, the conclusion to be taken is that fluorescent particles are generally the same size as non-fluorescent particles. The most common sizes for fluorescent particles are 0.7 to 0.9 μm and the total range of sizes is between 0.5 and 6 μm. A high probability of these results reflecting a majority of biogenic particles was discussed.

Particle fractions were talked through and the main insights that we gained were that AB and B type particles are dominant through the entire year, in clean periods, and AB type particles are clearly dominant in polluted periods, supporting a previously published hypothesis.

Finally, wind was seen as a possible mechanism to lift snow and sea particles, making them possible local sources of bioaerosols.

Further studies need to be made in the bioaerosols field to better understand their influence on cloud formation processes and their sources.

Acknowledgments

Firstly, I would like to thank my supervisors, Professor Doctor Julia Schmale and Professor Doctor Arsénio Fialho, for all the patience, guidance, wisdom, knowledge, support and kindness given throughout this past year. I would also like to express all the gratitude in the world to all my Extreme Environments Research Laboratory (EERL) colleagues (Ivo, Lubna, Hélène, Roman and Andrea) for all they did for me, from helping me after hours, to all their advice and expertise towards life and work. I leave here a special appreciation to Ivo, who was always there when I needed. I would also like to thank Doris and Cathie for all the affection and all their patience with the bureaucracies. I will never know how to thank my friends for being there, by my side, every step of the way. Leonor, Bismarck, Pranav, Sofi, Pati and Paula Cristina, you are the reason I could go through this journey with all my brain capacities intact, after all the problems, struggles and dilemmas. Miguel, you will always deserve a warming and very grateful hug. You were my partner in this walk.

Lastly, but definitely not the least, I would like to express my immense gratitude to my grandparents (Avó Céu and Avô Tó), to my gradmother (Avó Gusta), to my aunts (Tia Ferreira and Tia Lisa), to Naninha, to my uncles and cousins (Tio Luís, Tia Teresa, Pi and Mariana) and to titi São, who never once doubted my potential and helped me throughout all my academic life with unconditional love and support. Without all of you, I would have never been able to stand where I am today. To my grandfather, my dear Avô Gildo, you are still the light in me that gives me strength in all the important moments. A final and special thanks to my mom, dad, and brother: you taught me that one does not accomplish great things alone, and you were always (and will always be) by my side, thank you.

References

Andreae, M. O., & Gelencsér, A. (2006). Black carbon or brown carbon? the nature of light-absorbing carbonaceous aerosols. *Atmospheric Chemistry and Physics*, *6*(10), 3131–3148. https://doi.org/10.5194/acp-6-3131-2006

Ariya, P. A., Sun, J., Eltouny, N. A., Hudson, E. D., Hayes, C. T., & Kos, G. (2009). Physical and chemical characterization of bioaerosols - Implications for nucleation processes. In *International Reviews in Physical Chemistry* (Vol. 28, Issue 1). https://doi.org/10.1080/01442350802597438

Droplet Measurement Technologies. (n.d.). *WIBS-NEO TOOLKIT Operator Manual*.

Hartmann, M., Blunier, T., Brügger, S. O., Schmale, J., Schwikowski, M., Vogel, A., Wex, H., & Stratmann, F. (2019). Variation of Ice Nucleating Particles in the European Arctic Over the Last Centuries. *Geophysical Research Letters*, *46*(7), 4007–4016. https://doi.org/10.1029/2019GL082311

Heintzenberg, J., Okada, K., & Ström, J. (1996). On the composition of non-volatile material in upper tropospheric aerosols and cirrus crystals.

Atmospheric Research, *41*(1), 81–88. https://doi.org/10.1016/0169-8095(95)00042-9

Moallemi, A., Landwehr, S., Robinson, C., Simó, R., Zamanillo, M., Chen, G., Baccarini, A., Schnaiter, M., Henning, S., Modini, R. L., Gysel-Beer, M., & Schmale, J. (2021). Sources, Occurrence and Characteristics of Fluorescent Biological Aerosol Particles Measured Over the Pristine Southern Ocean. *Journal of Geophysical Research: Atmospheres*, *126*(11), 1–24. https://doi.org/10.1029/2021JD034811

Overland, J. E., Wood, K. R., & Wang, M. (2011). Warm Arctic-cold continents: Climate impacts of the newly open arctic sea. *Polar Research*, *30*(SUPPL.1), 1–14. https://doi.org/10.3402/polar.v30i0.15787

Pithan, F., & Mauritsen, T. (2014). Arctic amplification dominated by temperature feedbacks in contemporary climate models. *Nature Geoscience*, *7*(3), 181–184. https://doi.org/10.1038/ngeo2071

Quinn, P. K., Shaw, G., Andrews, E., Dutton, E. G., Ruoho-Airola, T., & Gong, S. L. (2007). Arctic haze: Current trends and knowledge gaps. *Tellus, Series B: Chemical and Physical Meteorology*, *59*(1), 99–114. https://doi.org/10.1111/j.1600-0889.2006.00236.x

Savage, N. J., Krentz, C. E., Könemann, T., Han, T. T., Mainelis, G., Pöhlker, C., & Alex Huffman, J. (2017). Systematic characterization and fluorescence threshold strategies for the wideband integrated bioaerosol sensor (WIBS) using size-resolved biological and interfering particles. *Atmospheric Measurement Techniques*, *10*(11), 4279–4302. https://doi.org/10.5194/amt-10-4279-2017

Schmale, J., Zieger, P., & Ekman, A. M. L. (2021). Aerosols in current and future Arctic climate. *Nature Climate Change*, *11*(2), 95–105. https://doi.org/10.1038/s41558-020-00969-5

Serreze, M. C., & Barry, R. G. (2011). Processes and impacts of Arctic amplification: A research synthesis. *Global and Planetary Change*, *77*(1–2), 85–96. https://doi.org/10.1016/j.gloplacha.2011.03.004

Vavrus, S., Holland, M. M., & Bailey, D. A. (2011). Changes in Arctic clouds during intervals of rapid sea ice loss. *Climate Dynamics*, *36*(7), 1475–1489. https://doi.org/10.1007/s00382-010-0816-0

Wu, G., Wan, X., Ram, K., Li, P., Liu, B., Yin, Y., Fu, P., Loewen, M., Gao, S., Kang, S., Kawamura, K., Wang, Y., & Cong, Z. (2020). Light absorption, fluorescence properties and sources of brown carbon aerosols in the Southeast Tibetan Plateau. *Environmental Pollution*, *257*, 113616. https://doi.org/10.1016/j.envpol.2019.113616